SEPARATED SHEET FLOWS

B.S. Yoon, Y.A., Semenov

School of Naval Architecture and Ocean Engineering University of Ulsan, Republic of Korea
E-mail: bsyoon@ulsan.ac.kr, semenov@a-teleport.com

ABSTRACT

A steady sheet flow of an inviscid incompressible fluid along a curvilinear surface ending with an arbitrarily shaped obstacle is considered in the presence of gravity. The effect of surface tension is ignored. The formulation of the problem is applicable to the study of free surface flows over obstacles in channels, weir flows, and pouring flows. An advanced hodograph method is employed for solving the problem, which is reduced to a system of integro-differential equations in the velocity modulus on the free surfaces and in the slope of the bottom surface. These equations are derived from the dynamic and kinematic boundary conditions. The Brillouin–Villat criterion is applied to determine the location of the point of flow separation from the rounded spout. Results concerning the effect of gravity on the flow detachment and the geometry of the free boundaries are presented over a wide range of Froude numbers including both the subcritical and the supercritical flow regimes. It is shown that there are two types of pouring flows for $F > 1$, one of which can be considered as the limiting flow configuration corresponding to the maximum height of the obstacle at the end of the channel.

1. INTRODUCTION

Sheet flows of an inviscid incompressible liquid have several applications, such as channel flows with obstructions, pouring flows, flows over weirs and spillways, and flows around nozzles, which are presented in the literature separately. Gravity in these problems plays an important role as a driving mechanism of motion.

The problem of channel flows with a semicircular submerged obstruction was studied using the boundary integral method by Forbes & Schwartz [1] and Vanden-Broeck [2]. The series truncation method was applied to a channel flow with a triangular obstruction by Dias & Vanden-Broeck [3-4]. Weir and pouring flows were studied by Vanden-Broeck & Keller [5 – 7] and Dias & Christodoulides [8].

In this paper, we consider nonlinear analytic solutions of steady sheet flows of an inviscid incompressible fluid along an arbitrarily shaped curvilinear channel bottom ending with an obstacle in the presence of gravity. This formulation naturally corresponds to pouring flows and flows over weirs. However, if we take into consideration the sufficiently large region of the upstream flow and place the obstacle far from the end of the channel specifying the boundary condition far downstream, we will obtain the boundary conditions corresponding to flows in an infinite channel with obstructions.

The key step of our hodograph method is the analytical construction of two governing functions: the complex velocity and the derivative of the complex potential, which are defined in an auxiliary parameter region. The details of the method and the new methodology for constructing the governing functions are presented in the paper by Semenov & Yoon [9]. By using this methodology, all one has to do is to specify boundary conditions for the complex velocity function, which are easy to obtain from the kinematic and dynamic boundary conditions, and then apply the integral formula that solves the mixed boundary-value problem in order to derive an expression for the complex velocity function. The second expression, i.e. that for the derivative of the complex potential for channel flows is well-known and can be obtained using a classical conformal mapping method.

2. STATEMENT OF THE PROBLEM

We consider the steady, two-dimensional potential flow of an inviscid, incompressible fluid along a curvilinear bottom, BO, ending with a circular cylinder of radus R sketched in Fig. 1*a*. Far upstream, the flow is uniform, with constant velocity U and fixed depth H. The fluid is subject to the downward acceleration of gravity g, and the disturbing height of the bottom W can be located arbitrarily far upstream from the end of the channel. At point O the sheet flow separates from the bottom surface and falls down under gravity.

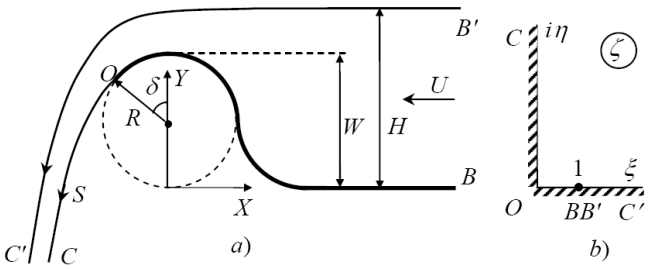

Figure 1. Sketch of the sheet flow *a*) and the parameter region *b*)

Following Wanden-Broeck & Keller [5], we introduce $L = \left(Q^2 / g\right)^{\frac{1}{3}}$ as the unit length and $V = \left(Qg\right)^{\frac{1}{3}}$ as the unit

velocity, where the discharge $Q = UH$. The dimensionless discharge $q = Q/VL = uh$ is equal to 1, where $u = U/V$ and $h = H/L$ are the dimensionless velocity and thickness of the liquid layer. By using these definitions we can express the Froude number

$$F = \frac{U}{\sqrt{gH}} = u^{3/2} \tag{1}$$

and the velocity magnitude on the free surface determined using the Bernoulli equation assuming the pressure on the free surface to be constant

$$v = u\sqrt{1 + \frac{2(1 - y/h)}{F^2}}\,. \tag{2}$$

Let the first quadrant of the ς-plane, where the complex variable is $\varsigma = \xi + i\eta$, correspond to the flow region in the physical plane. Conformal mapping allows us to choose the location of three points *O*, *C* and *B* as shown in Figure 1*b*. Then, the interval $0 < \xi < 1$ of the real axis corresponds to the bottom of the channel, the interval $1 < \xi < \infty$ corresponds to the upper free surface $B'C'$, and the imaginary η-axis of the parameter region corresponds to the free boundary OC. We introduce the complex potential $w = \phi + i\psi$ where ϕ is the flow potential and ψ is the stream function. The solution of the problem is sought in parametric form by determining two functions, which are the complex conjugate velocity, dw/dz, and the derivative of the complex potential, $dw/d\varsigma$, both defined in the parameter region ς. Once expressions for these functions have been determined, the solution of the problem, i.e. the flow boundaries and the velocity field in the flow region is determined as follows

$$z(\varsigma) = z_0 + \int_0^{\varsigma} \frac{dw/d\varsigma'}{dw/dz}\, d\varsigma'\,, \tag{3}$$

where z_0 is the coordinate of point O.

2.1. Governing expressions

The expressions for the complex potential and its derivative are as follows

$$w = \frac{q}{\pi}\ln(1 - \varsigma^2)\,, \qquad \frac{dw}{d\varsigma} = \frac{2q}{\pi}\frac{\varsigma}{\varsigma^2 - 1}\,. \tag{4}$$

In order to derive an expression for the complex velocity, we assume that the magnitude of the velocity v and its argument $\gamma = -\beta_i$, $i = 1, 2$, where β_1 is the slope of the bottom surface and β_2 is the slope of the upper free surface $B'C'$, are known as functions of the parametric variables η and ξ, respectively. Using the above definitions, the boundary conditions for the complex velocity function dw/dz can be written as follows

$$\begin{aligned} &\arg\left(\frac{dw}{dz}\right) = \gamma(\xi) = \begin{cases} -\beta_1(\xi), & 0 < \xi < 1, \quad \eta = 0, \\ -\beta_2(\xi), & 1 < \xi < \infty, \quad \eta = 0. \end{cases} \\ &\left|\frac{dw}{dz}\right| = v(\eta), \qquad\qquad 0 < \eta < \infty, \quad \xi = 0. \end{aligned} \tag{5}$$

The final expression for the complex velocity can be rewritten as follows

$$\frac{dw}{dz} = v_0 \exp\left[\begin{array}{l} \left\{\displaystyle\int_0^1 \frac{d\beta_1}{d\xi} + \int_1^{\infty} \frac{d\beta_2}{d\xi}\right\} \frac{1}{\pi}\ln\left(\frac{\xi' - \varsigma}{\xi' + \varsigma}\right) d\xi' \\ -\dfrac{i}{\pi}\displaystyle\int_0^{\infty} \frac{d\ln v}{d\eta'}\ln\left(\frac{i\eta' - \varsigma}{i\eta' + \varsigma}\right) d\eta' - i\beta_0 \end{array}\right]. \tag{6}$$

where $v_0 = v(0)$ and $\beta_0 = \beta(0) = \pi + \delta$ are the velocity magnitude and angle at point O.

The unknown functions $\beta_1(\xi)$, $\beta_2(\xi)$, and $v(\eta)$ are derived from the dynamic and kinematic boundary conditions, which lead to a system of integro-differential equations. The Brillouin–Villat criterion is applied to determine the location of the point of flow separation from the rounded spout.

3. ANALYSIS OF SHEET FLOWS WITH OBSTRUCTIONS

3.1. Validation of the method. Channel flows.

For validation purposes, we consider steady channel flows over a triangular obstacle at the channel bottom. In Fig. 2*a* the free-surface profiles obtained using the present method are shown and compared with the corresponding solution of Dias and Vanden-Broeck [3] for height of the triangle *W/L*=0.48 and Froude number *F*=1.52. This solution represents the limiting flow configuration corresponding to the perturbation of the soliton wave for which the velocity at the point of maximum elevation tends to zero and the angle between the free surfaces at the right and at the left tends to 120^0.

The free surface profile corresponding to a subcritical upstream flow and a supercritical downstream flow is shown in Figure 2*b*. As is seen, both obtained solutions in Figures 2 and 3 (solid line) agree quite well with the solutions of Dias and Vanden-Broeck [3].

The present formulation of the problem allows us to consider an arbitrarily shaped channel bottom. The effect of

the obstacle shape on the free surface profile is shown in Fig. 3 for the case of a uniform flow perturbed by an obstacle. For the obstacle shown by the dashed line the straight part is absent (B=0), while for that shown by the solid line the length of the straight part is equal to H (B=H). The radius R=H, and the obtained Froude number is F=1.6. It can be seen that the width of the obstacle affects the height of the wave.

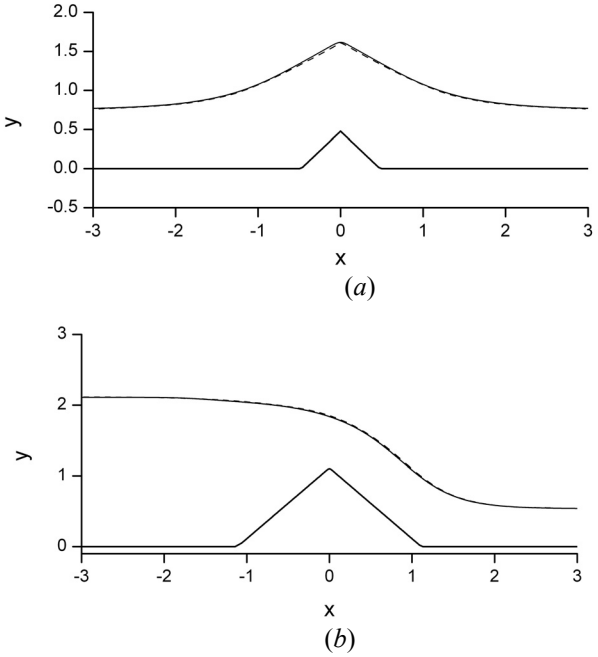

Figure 2. Obtained results (solid line) compared with the results of Dias and Vanden-Broeck [3] (dashed line).

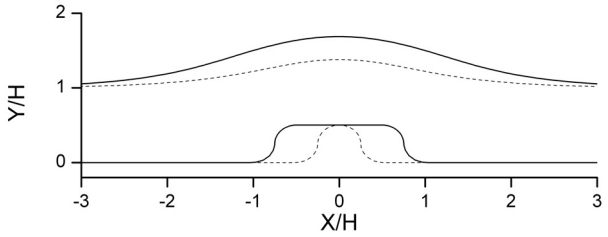

Figure 3. Effect of the obstacle length on the free-surface profile for height W/H=0.5 and Froude number F=1.6.

Fig. 4 shows the relative maximum elevation

$$\tau = \frac{y_{\max}}{h} - 1$$

of the free surface versus Froude number F for two values of the relative height $\alpha = W/H$ and three various shapes of the obstacle. These results are similar to those presented in the papers by Vanden-Broeck [2] and Dias & Vanden-Broeck [3] for semicircular and triangular obstacles, respectively. For a given α and shape of the obstacle there exists some minimum Froude number F^* for which a solution of the problem is unique. In the range $F^* < F < F^{**}$ there are two solutions corresponding to a uniform flow and a soliton wave perturbed by the obstacle. Here, F^{**} is the Froude number corresponding to the limiting configuration of the perturbed soliton wave with a stagnation point at the top of the wave. As can be seen from Fig. 4, increasing the length of the obstacle shifts the range $F^* < F < F^{**}$ to larger values of F^* and F^{**}.

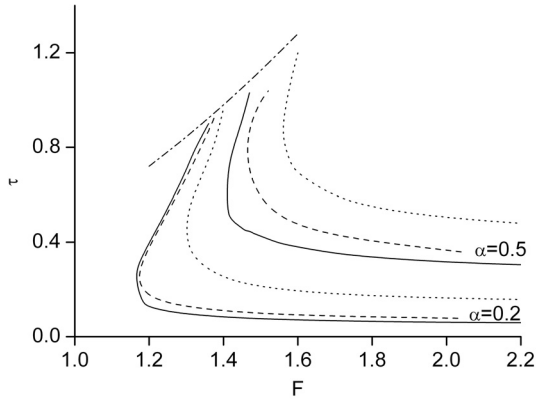

Figure 4. Effects of the obstacle shape and height $\alpha = W/H$ on the maximum elevation τ of the free surface versus Froude number: the solid lines correspond to the obstacle shown by the dashed line in Fig. 3; the dashed lines correspond to the semicircular obstruction [2]; the dotted lines correspond to the obstacle shown in Figure 3 by the solid line.

3.2. Pouring and weir flows

Fig. 5 shows the free surface profiles for subcritical flows over a bottom surface consisting of two circular arcs of radius $R = H$. The length of each circular arc for cases (*a*) and (*c*) is the same and equal to $S_1 = R\delta_1$, where $\delta_1 = \arccos[W/(2R)]$. For cases (*b*) and (*d*) the length of the second circular arc from which the flow separates, is equal to $S_2 = R\delta_2$, where $\delta_2 = \delta_1 + \delta$ and δ is the angle of flow separation from the cylindrical spout. In Figs. 7*b* and 7*d* only the wetted part of the cylindrical spout is shown. For cases (*a*) and (*c*) the curvature of the free surface at the point of flow detachment is infinite while for the smooth separation it is equal to the curvature of the spout -1/*R*.

The flows shown in Fig. 5 are similar to flows over weirs for which the discharge Q is determined by the height of the free surface $H - W$ and the cross-sectional area $A = (H - W)B$ above the weir of width B

$$Q = C_q \sqrt{g(H-W)}A\,.$$

The discharge coefficient C_q in the case of two-dimensional flows can be expressed as follows

$$C_q = F\left(\frac{H-W}{H}\right)^{-\frac{3}{2}} = F\left(\frac{H-W}{W}\right)^{-\frac{3}{2}}\left(\frac{W}{H}\right)^{-\frac{3}{2}}.$$

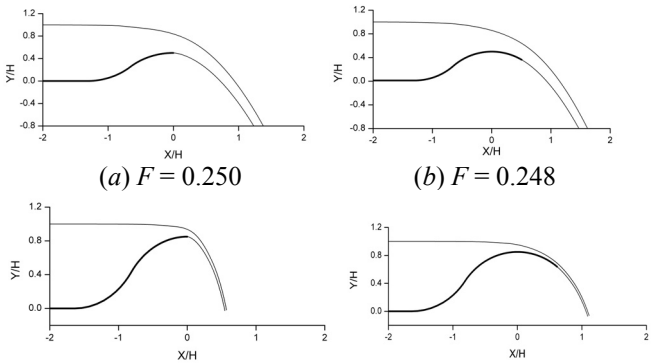

(*a*) $F = 0.250$ (*b*) $F = 0.248$

(*c*) $F = 0.0351$ (*d*) $F = 0.0336$

Figure 5. Free surface profiles of sheet subcritical flows with a fixed point of flow separation [(*a*) and (*c*)] and smooth flow detachment from the cylindrical spout [(*b*) and (*d*)]. The height of the obstacle *W/H*=0.5 for (*a*) and (*b*) and *W/H*=0.85 for (*c*) and (*d*).

Fig. 6 shows the discharge coefficient multiplied by $(H/W)^{-\frac{3}{2}}$ as a function of the ratio $(H-W)/W$ for a channel shaped as shown in Figures 5*a* and *c* (solid line) and Figures 5*b* and *d* (dashed line). The results of Vanden-Broeck & Keller [5] for thin weirs are also shown by solid squares. It can be seen that the shape of the weir affects the discharge coefficient only slightly. Due to this fact our results for the weir without a rounded spout agree with the results obtained by Vanden-Broeck & Keller [5] for thin weirs.

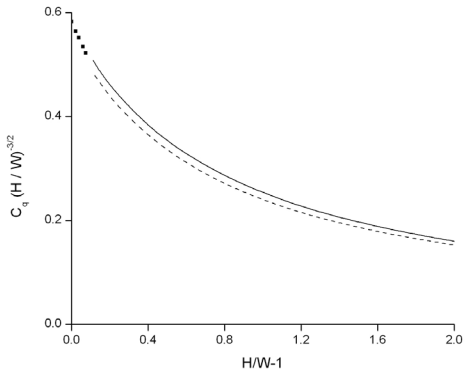

Figure 6. $C_q (H/W)^{-3/2} = F((H-W)/W)^{-3/2}$ versus $H/W - 1$ for variously shaped channels

The Froude number dependence of the height of the obstruction is shown in Fig. 7 for pouring flows (solid line) and compared with the results corresponding to channel flows (dashed line) taken from Dias & Vanden-Broeck [5]. Although the geometry of the obstacles in the present calculations is quite different from triangles used in [5] for channel flows, the results both for the channel and the pouring flows are in fairly good agreement with each other for Froude numbers $F < 0.8$. The difference in the range $0.8 < F < 1$ shows the effect of the channel end on the whole of the flow. The solid line in Fig. 7 corresponds to pouring flows with a uniform inflow velocity, which for Froude numbers $F > 1$ can be considered as the limiting flow configuration corresponding to the maximum height of the obstacle W^* for a given Froude number. A second type of pouring flows occurs at smaller heights of the obstacle in the range $0 < W < W^*$, for which the uniform inflow condition is satisfied asymptotically.

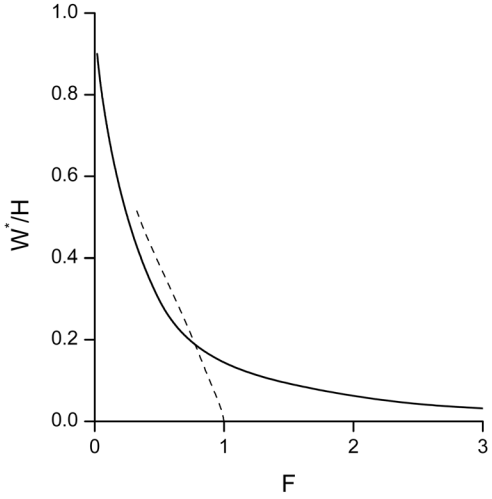

Figure 7. Height of the obstruction versus Froude number for pouring flows (solid line) and for the open channel flows (dashed line) taken from Dias & Vanden-Broeck [5].

4. REFERENCES

1. Forbes, L.K. & Schwartz, L.W. 1982 Free-surface flow over a semicircular obstruction. J. Fluid Mech. **114**, 299 – 314.
2. Vanden-Broeck, J.-M. 1987 Free-surface flow over an obstruction in a channel. Phys. of Fluids, **30**, 2315 – 2317.
3. Dias, F. & Vanden-Broeck, J.-M. 1989 Open channel flows with submerged obstructions. J. Fluid Mech. **206**, 155 – 170.
4. Dias, F. & Vanden-Broeck, J.-M. 2002 Generalised critical free-surface flows. J. Engng Maths **42**, 291–301, 2002.
5. Vanden-Broeck, J.-M. & Keller, J.B. 1987. Weir flows. J. Fluid Mech. **176**, 283 – 293.
6. Vanden-Broeck, J.-M. & Keller, J.B. 1986 Pouring flows. Phys. of Fluids, **29**, 3958 – 3961.
7. Vanden-Broeck, J.-M. & Keller, J.B. 1988 Pouring flows with separation. Phys. of Fluids A, **1**, 150 – 158.
8. Dias, F. and Christodoulides, P. 1991 Ideal jets falling under gravity. Phys. of Fluids A, **3**, 1711 – 1717.
9. Semenov, Y.A., Yoon B.S. 2009 Onset of Flow Separation at Oblique Water Impact of a Wedge. Physics of Fluids, **21**, pp. 112103 - 11.